

# Numerical Simulation of Droplet Impact on Patterned Surfaces

H.B. Parizi, L. Rosenzweig, J. Mostaghimi, S. Chandra, T. Coyle, H. Salimi, L. Pershin, A. McDonald, and C. Moreau

(Submitted March 10, 2007; in revised form July 24, 2007)

This work presents numerical simulation results for molten nickel and zirconia (YZS) droplets impacting on different microscale-patterned surfaces of silicon. The numerical simulation clearly showed the effect of surface roughness and solidification on the shape of the final splat, as well as the pore creation beneath the sprayed material. Simulations were performed using computational fluid dynamic software, SimDrop. The code uses a three-dimensional finite-difference algorithm solving the full Navier-Stokes equation, including heat transfer and phase change. A volume of fluid (VOF) tracking algorithm is used to track the droplet-free surface. Thermal contact resistance at the droplet-substrate interface is also included in the model. Specific attention is paid to the simulation of droplet impact under plasma spraying conditions. Droplet sizes ranged from 15 to 60 microns with initial velocities of 70–250 m/s. Substrate surfaces were patterned with regular arrays of cubes 1–3  $\mu\text{m}$  high, spaced either 1  $\mu\text{m}$  or 5  $\mu\text{m}$  from each other. Different splat morphologies produced by simulations are compared with those obtained from the experiment conducted under the same impact and surface conditions.

**Keywords** droplet impact, numerical simulation, patterned surface, solidification, thermal spray coating

## 1. Introduction

Liquid-droplet spreading on surfaces occurs in many industrial processes such as painting, coating, ink jet printing, lubrication, and thermal spraying. In this process, in order to enhance the adhesion of the impact droplets on the surface, the substrate is usually grit-blasted. Therefore, the complex physical phenomena of droplet spreading and solidification take place on a microscopically rough substrate. The surface roughness of the substrate affects the dynamics of droplet spread and consequently the shape and the thickness of the final splat. Increasing surface roughness promotes splashing of impacting molten droplets, which in turn increases the roughness of coating layers formed by solidified splats. Therefore, the initial roughness of the surface may affect the porosity of thermal spray coatings.

This article is an invited paper selected from presentations at the 2007 International Thermal Spray Conference and has been expanded from the original presentation. It is simultaneously published in *Global Coating Solutions, Proceedings of the 2007 International Thermal Spray Conference*, Beijing, China, May 14–16, 2007, Basil R. Marple, Margaret M. Hyland, Yuk-Chiu Lau, Chang-Jiu Li, Rogerio S. Lima, and Ghislain Montavon, Ed., ASM International, Materials Park, OH, 2007.

**H.B. Parizi**, Simulent Inc., 203 College Street, Suite 302, M5T 1P9 Toronto, ON, Canada; **L. Rosenzweig**, GE Global Research, New York, USA; **J. Mostaghimi**, **S. Chandra**, **T. Coyle**, **H. Salimi**, **L. Pershin**, and **A. McDonald**, University of Toronto, Toronto, ON, Canada; and **C. Moreau**, National Research Council Canada, Boucherville, QC, Canada. Contact e-mail: parizi@simulent.com.

Though many experimental and numerical studies have been presented on droplet impact and solidification processes, only a few of them considered the effect of surface roughness (Ref 1). Using a two-dimensional axi-symmetric model, Ahmed and Rangel (Ref 2) numerically studied the impact and solidification of an aluminum droplet on a wavy substrate. The average size of the droplets under their study was 600  $\mu\text{m}$  with an impact velocity of 100 m/s. Their results show that droplet impact on an uneven substrate is almost always accompanied by splashing, which would be diminished by increasing surface roughness. Fukunuma (Ref 3) presented a formula that describes the flattening process of a droplet on a rough surface, and concluded that the flattening ratio and the flattening time decreases with increasing roughness. Liu et al. (Ref 4) numerically studied the impact of tungsten droplets on substrates with wavy surfaces for droplet sizes of 10–60  $\mu\text{m}$ , impact velocities of 50–400 m/s and a range of Weber and Reynolds numbers to account for the effect of varying viscosity and surface tension. However, their two-dimensional axi-symmetric model did not include solidification. They found that for wavelengths of the surface roughness larger than the droplet diameter, droplet spreading ended with breakup. Raessi et al. (Ref 1) used a three-dimensional model (Ref 5, 6) to numerically simulate the effect of surface roughness on the impact dynamics and the splat shape of a 40  $\mu\text{m}$  alumina droplet impinging on a substrate with a velocity of 65 m/s. The surface was alumina which was patterned by cubes were regularly spaced at an interval twice their size. Three different cube sizes, of 1, 2, and 3  $\mu\text{m}$ , were used. They concluded that droplet solidification is the main mechanism responsible for changing splat shape.

In this study the three-dimensional numerical modeling of deformation and interaction of molten nickel and zirconia (YSZ) droplets impinging and solidifying on a

textured (patterned) surface during thermal spraying is presented. One of the principal objectives of this study is to simulate pore formation in thermal spray coatings due to incomplete filling of cavities in a rough substrate, and to determine the effect of processing parameters on the morphology of splats formed by the impact of both metal (nickel) and ceramic (zirconia) droplets.

## 2. Numerical Model

### 2.1 Fluid Flow

Bussmann et al. (Ref 5) have presented a detailed discussion of the fluid flow algorithm that is used in the three-dimensional code, SimDrop (Ref 7). Fluid flow for droplet impact was modeled using a finite-difference solution of the Navier-Stokes equations in a three-dimensional Cartesian coordinate system. The liquid is assumed to be incompressible and any effect of the ambient air on droplet impact dynamics is neglected. The fluid flow is assumed to be laminar. The free surface of the deforming droplet is tracked using the volume of fluid (VOF) scheme described in (Ref 5). In this method, a scalar function  $f$  is defined as the fraction of a cell volume occupied by the fluid.  $f$  is assumed to be unity when a cell is fully occupied by the fluid and zero for an empty cell. Cells with values of  $0 < f < 1$  contain a free surface. Surface tension was modeled as volumetric force acting on fluid near the free surface; the method used was the continuum surface force (CSF) model integrated with smoothed values of function  $f$  in evaluating free surface curvature. Tangential stresses at the free surface were neglected. Contact angles were applied as a boundary condition at the contact line.

### 2.2 Heat Transfer

Heat transfer in the droplet and substrate was modeled by solving the energy equation, neglecting viscous dissipation. Passandideh-Fard et al. (Ref 6) presented more details about this model. Heat transfer in the droplet and substrate regions were coupled through the heat flux  $q$  at the droplet-substrate interface. For the portions of the substrate not covered by the droplet it is assumed that there was no heat transfer so that  $q = 0$ , where the droplet and substrate are in contact, the following relationship was used:

$$q = \frac{(T - T_W)_{\text{Substrate}}}{R_C} \quad (\text{Eq 1})$$

where  $R_C$  is the thermal contact resistance between droplet and substrate per unit area,  $T$  and  $T_W$  are the local temperatures of droplet and substrate, respectively. Values of  $R_C$  are provided as an input to the model. In principle thermal contact resistance,  $R_C$ , depends on the droplet material, impact surface material and characteristics (whether it is smooth or rough or has contamination), and could vary with both time and position of the impact. However, in this study a constant value was used

in all simulations. When the average experimental value for the thermal contact resistance was available, that value was used in the simulations. Otherwise, through a trial and error procedure, the best value is obtained from comparing the simulation results with the experimental observations.

Liquid density and surface tension were assumed constant. The effect of varying density has been investigated by Raessi et al. (Ref 8) for the very low-speed impacts. They showed that by using different (though constant) values of solid and liquid density, shrinkage may be observed that will affect the size of cavities. Liquid viscosity and substrate thermal properties, however, were assumed to vary with temperature. Properties of nickel and silicon are well documented (Ref 9), but properties for molten YSZ droplet are less investigated. The values presented by Shinoda et al. (Ref 10) and Simon and Pal (Ref 11) have been used in this work.

### 2.3 Governing Equations

Equations of conservation of mass and momentum for the flow are:

$$\nabla \cdot \mathbf{V} = 0 \quad (\text{Eq 2})$$

$$\frac{\partial \mathbf{V}}{\partial t} + \nabla \cdot (\mathbf{V} \mathbf{V}) = -\frac{1}{\rho} \nabla p + \nabla^2 \nu \mathbf{V} + \frac{1}{\rho} \mathbf{F}_b \quad (\text{Eq 3})$$

where  $\mathbf{V}$  represents the velocity vector,  $p$  the pressure,  $\rho$  the density,  $\nu$  the kinematic viscosity, and  $\mathbf{F}_b$  any body forces acting on the fluid, including the surface forces.

By neglecting viscous dissipation and assuming that the densities of liquid and solid are constant at melting point and equal to each other, the energy equation can be represented by:

$$\frac{\partial h}{\partial t} + (\mathbf{V} \cdot \nabla)h = \frac{1}{\rho} \nabla \cdot (k \nabla T) \quad (\text{Eq 4})$$

where  $h$  is the enthalpy of the fluid,  $k$  is the thermal conductivity, and  $T$  is the temperature. Since the scalar function  $f$  is passively advected with the flow,  $f$  should satisfy the advection equation as well:

$$\frac{\partial f}{\partial t} + (\mathbf{V} \cdot \nabla)f = 0. \quad (\text{Eq 5})$$

Given the volumetric nature of  $f$  and in order to maintain a sharp interface, the discretization of the above equation requires special treatment. Youngs' algorithm is used to track the free surface. It consists of two steps: an approximate reconstruction of the interface followed by a geometrical evaluation of volume fluxes across cell faces. More details about the numerical approach to solve the governing equations can be found in (Ref 1, 5, 6, 8).

The governing equations were solved implementing a finite-volume technique and a three-dimensional Cartesian structured grid. For all the simulations, due to existence of symmetric boundaries, only a quarter of the domain has been considered and therefore the problem size was reduced and computational time was saved. Along symmetric boundaries, free slip, no penetration

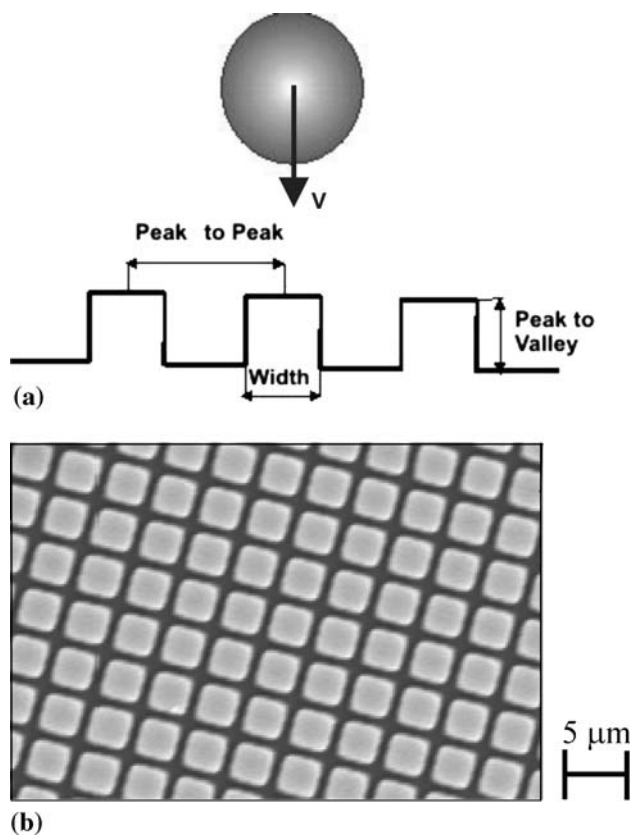


**Fig. 1** (a) Schematic set up for simulation of the droplet impact on a patterned surface. The major parameters define the surface roughness are: Peak to peak distance, width, and peak to valley distance (height) of the cubes. Throughout this paper, “space” between cubes indicates the peak to peak minus the width of each cube. (b) SEM image of a typical textured silicon wafer

conditions, and adiabatic thermal boundary condition were applied. The grid size used in these calculations was between 0.3 and 1  $\mu\text{m}$ . The total number of cells per droplet radius in these calculations varied from 15 to 21, which is high enough to ensure grid independent results.

In Fig. 1(a), the schematic set up for the numerical simulation of a droplet impact on a uniform textured surface is shown. Though the roughness created on the surface by grit blasting is random, numerical modeling with a well-defined roughness model can provide valuable information about the spreading and solidification behavior of the droplet.

### 3. Experimental Parameters

In order to directly compare the simulation results with the experimental observation, the impact parameters for simulation were those used or measured in the experimental set ups.

The impact experiments for nickel droplets on textured silicon were performed at Industrial Materials Institute of

**Table 1** In-flight parameters for nickel particles as measured during experiments (a)

Nickel on textured silicon	1 $\mu\text{m}$ height 1 $\mu\text{m}$ space 4 $\mu\text{m}$ width	1 $\mu\text{m}$ height 5 $\mu\text{m}$ space 4 $\mu\text{m}$ width
Initial diameter, $\mu\text{m}$	50 $\pm$ 3	60 $\pm$ 3
Impact temperature, $^{\circ}\text{C}$	2390 $\pm$ 70	2225 $\pm$ 20
Impact velocity, m/s	70 $\pm$ 2	73 $\pm$ 2
Substrate temperature, $^{\circ}\text{C}$	350	350
Contact resistance, $\text{m}^2\cdot\text{K}/\text{W}$	5E-6 (b)	2E-6 (b)

(a) The average values of the in-flight parameters are shown for the particles on each specific wafer. The statistical errors of the mean are also shown with each average where available. Powder particles were sieved. (b) Average measured values

the National Research Council of Canada. The experiments were performed using an SG100 plasma torch. The powders were sieved with an average diameter shown in Table 1. The two-color pyrometry system was used to measure the radiation of the in-flight particles, from which particle temperature was calculated. More detailed descriptions of the experiments have been given in (Ref 12, 13).

The substrates were silicon wafers patterned by etching with micron-sized columns to make a textured rough surface. The column heights were 1  $\mu\text{m}$  and the spaces between the columns were either 1  $\mu\text{m}$  or 5  $\mu\text{m}$ . An SEM image of a typical textured silicon wafer used in these experiments is shown in Fig. 1(b). The wafers were heated to 350  $^{\circ}\text{C}$  during spraying. The contact resistance between the substrate and the splat was calculated by measuring the average cooling rate between splats and textured silicon wafers. The cooling rate was measured using two-color pyrometry system.

The experiments with zirconia were performed at the Center for Advanced Coating Technologies (CACT) at the University of Toronto. In-flight particle conditions upon impact were measured with a DPV-2000 monitoring system (Tecnar Automation Ltee, St-Bruno, Canada). It simultaneously measures the velocity and temperature of the particle and calculates its diameter. In these experiments too the sieved particles were used for deposition.

For footprint deposition on the patterned Si substrates a torch working on  $\text{CO}_2/\text{CH}_4$  gas mixture was used at the CACT. DPV scans of the particulate plume were performed before spraying. Spray distance of 50 mm was kept constant throughout the experiments. The footprints were collected on the patterned Si substrates which were kept at room temperature. After auto-center routine the center of the plume has temperature and velocity of  $T=2900$   $^{\circ}\text{C}$  and  $V=250$  m/s, respectively. These average velocity and temperature were also used for simulations as shown in Table 2, column (1). The values of thermal contact resistance are numerically obtained by comparing the simulation results and the experimental observation.

The substrates were silicon wafers with micron-sized columns of heights 3.3  $\mu\text{m}$  and 1.5  $\mu\text{m}$ . The spaces between the columns were 5  $\mu\text{m}$  and the width of columns equal to 4  $\mu\text{m}$ . The wafers were kept at room temperature during spraying.

**Table 2** Impact and surface parameters used in simulating zirconia particles

Zirconia on textured silicon	3.3 $\mu\text{m}$ height 1 $\mu\text{m}$ space 4 $\mu\text{m}$ width	1.5 $\mu\text{m}$ height 5 $\mu\text{m}$ space 4 $\mu\text{m}$ width	
	(1)	(2)	(3)
Initial diameter, $\mu\text{m}$	15	15	15
Impact temperature, $^{\circ}\text{C}$	2900	2700	2900
Impact velocity, m/s	250	250	250
Substrate temperature, $^{\circ}\text{C}$	25	25	30
Contact resistance, $\text{m}^2\cdot\text{K}/\text{W}$	1E-8	1E-7	1E-8

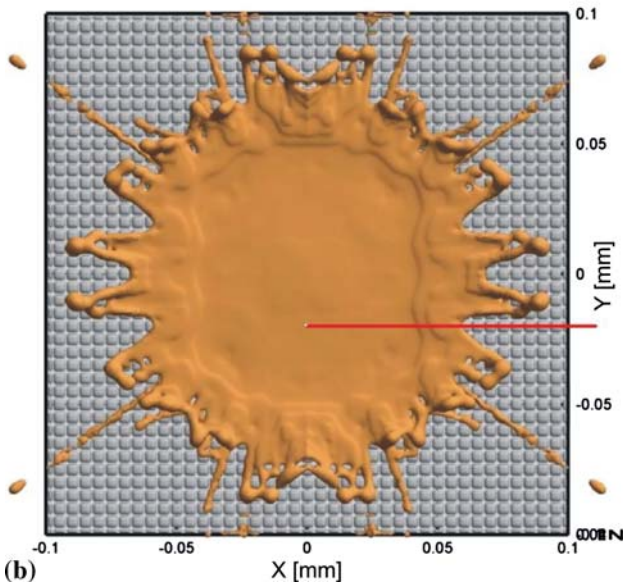
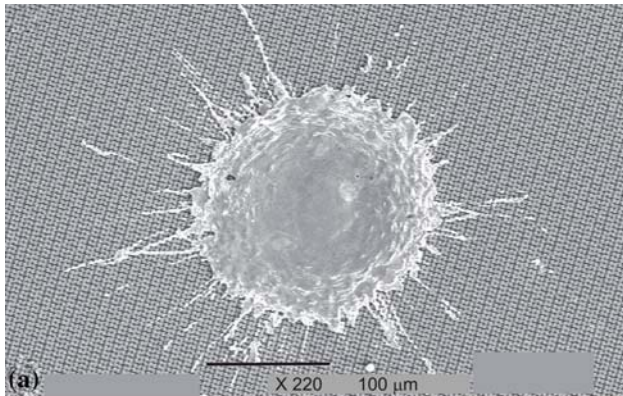


**Fig. 2** (a) An SEM image of the splat shape of nickel on silicon with 1  $\mu\text{m}$  high and 1  $\mu\text{m}$  spacing between the cubes, taken from experiments (Ref 12, 13). (b) Numerical result for a splat shape of nickel on silicon with the same conditions as experiments (a). Other impact parameters are stated in Table 1

## 4. Results and Discussions

### 4.1 Nickel Droplet Impact

Figure 2(a) shows an SEM image of nickel splat on 1  $\mu\text{m}$  height and 1  $\mu\text{m}$  spaced textured silicon surface. The

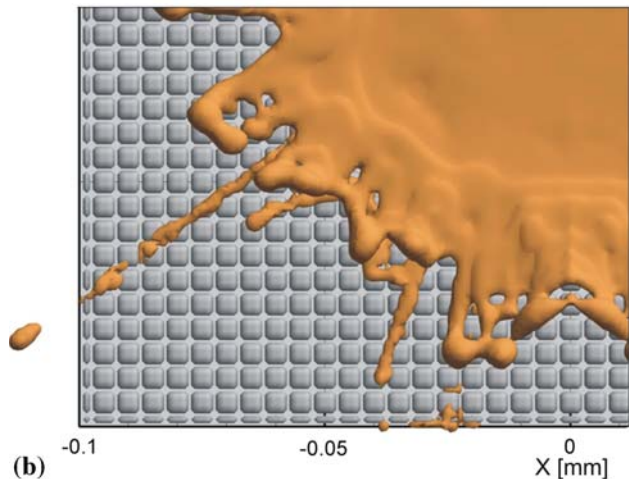
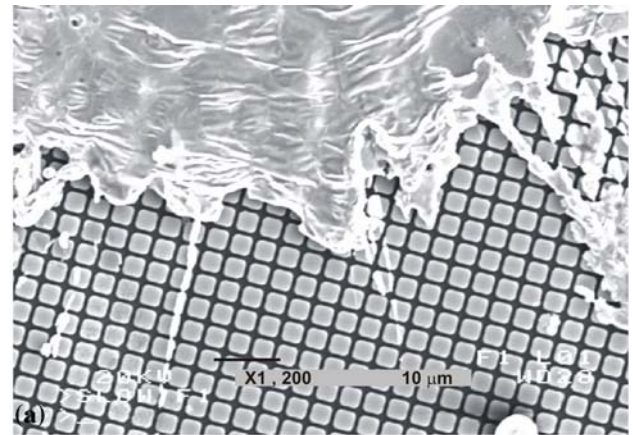


**Fig. 3** Close up of the splat shape at the rim of splat for Fig. 2: (a) Experiment and (b) Simulation

other experimental conditions are reported in Table 1. A top view of the simulation result for the same impact conditions is shown in Fig. 2(b). The close up images of the edge of splat for both experimental and simulation results are shown in Fig. 3(a) and (b), respectively.

The final splat diameter obtained from the simulation was 180  $\mu\text{m}$  which is comparable with the average value of 195  $\mu\text{m}$  that can be measured from the experiment (excluding all splashes). Figure 4(a) and (b) shows the SEM images and the numerical results, respectively, for nickel splat on 1  $\mu\text{m}$  height, 5  $\mu\text{m}$  spaced textured silicon. In Fig. 5(a) and (b), the close up of the splat SEM image and corresponding numerical simulation of the edge of the same splat are shown, respectively. The maximum diameter that can be measured from SEM was 175  $\mu\text{m}$  which is in good agreement with the calculated value of 170  $\mu\text{m}$ . All splash measurements were done by visually measuring the diameter of the splats (discarding the splashes) on the substrate.

Figure 6(a) shows a cross section of the splats and the substrate, at the location shown with a line in Fig. 2(b). As is seen from the figure, the cavities between the textured posts on the substrate are filled with the droplet material in the middle of the splat, whereas close to the boundaries

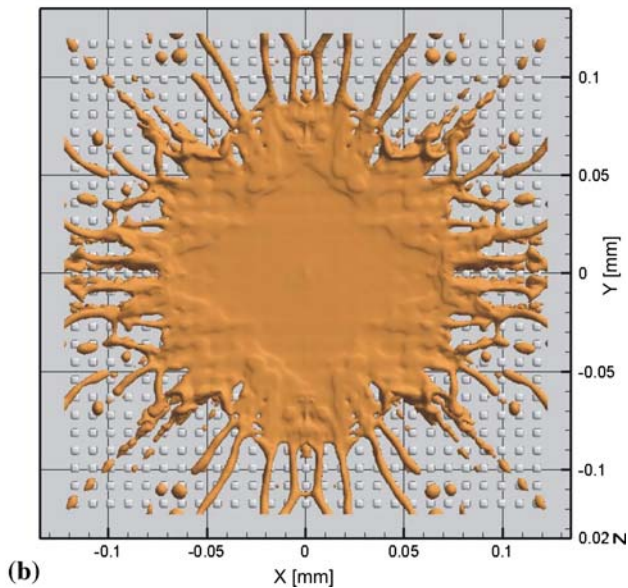
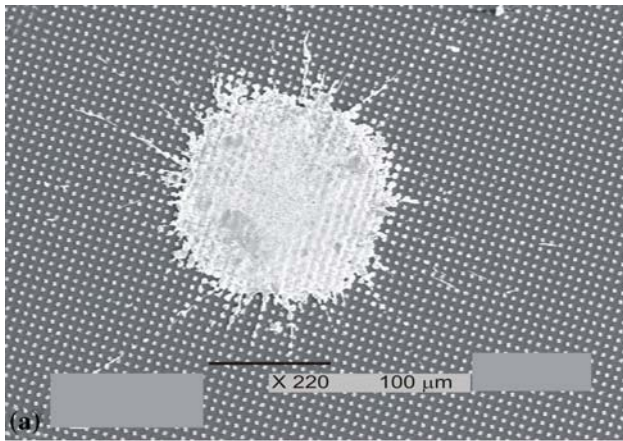
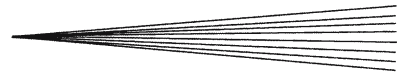


**Fig. 4** An SEM image of the splat shape of nickel on silicon with 1  $\mu\text{m}$  high and 5  $\mu\text{m}$  spacing between the cubes, taken from experiments (Ref 12, 13). (b) Numerical result for a splat shape of nickel on silicon with the same conditions as experiments (a). Other impact parameters are stated in Table 1

of the splat the cavities are partially filled or completely open. In Fig. 6(b), the focused ion beam (FIB) image of one nickel splat, sprayed almost under the same condition is shown. As can be seen from the close up image, most of the posts in the middle of the splat are also filled with nickel. This is a clear indication that close to the impact point of the droplet, where the kinetic energy of the liquid and its normal velocity are at highest, the cavities on the surface are filled up regardless of the size. As the normal velocity of the liquid reduces and liquid spreads in radial direction, the liquid energy is not enough anymore to fill the cavities.

#### 4.2 Zirconia Droplet Impact

Figure 7(a) shows the simulation results of a 15  $\mu\text{m}$  molten zirconia droplet impact on the textured silicon

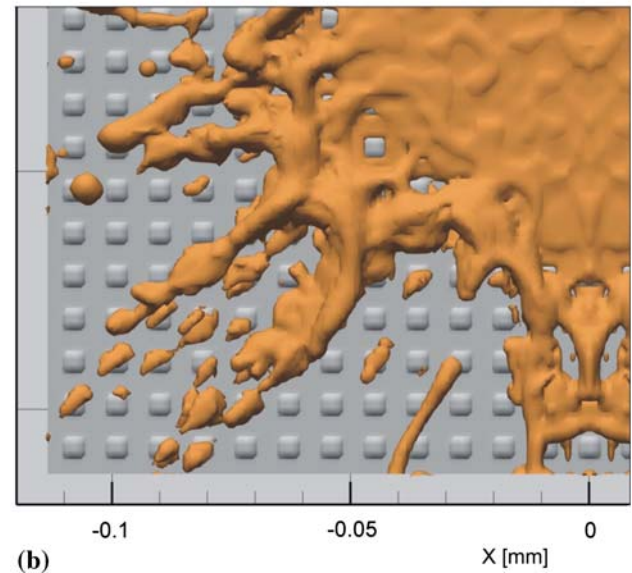
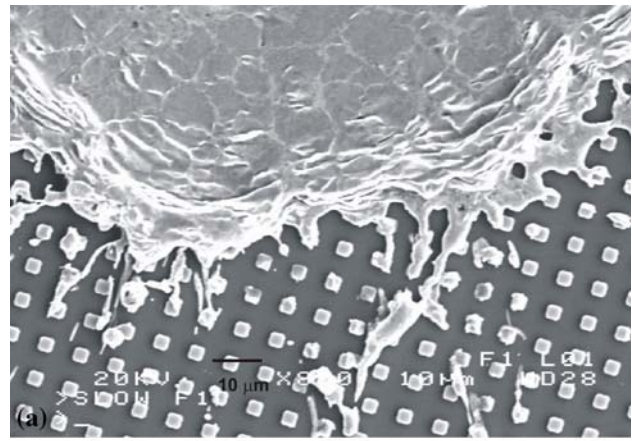


**Fig. 5** Close up of the splat shape at the rim of splat for Fig. 4: (a) Experiment and (b) Simulation

surface of 3.3  $\mu\text{m}$  height and 1  $\mu\text{m}$  space between cubes. Other impact conditions are stated in Table 2, column (1). Figure 7(b), shows the cross section of the splat at the location which is indicated with a line. The initial velocity of the droplet in this case was more than three times that of the nickel splat (250 m/s to be compared to 70 m/s). The roughness parameters, i.e., peak-to-peak, and peak-to-valley distances are comparable to the droplet size, i.e., 15  $\mu\text{m}$ . As can be seen the shape of the splat in this case is closer to a square than a circle and most of the cavities in between the roughness posts are filled with the material.

In Fig. 8(a), two sample SEM images of YSZ splats, sprayed at CACT under the same conditions (listed in Table 2, column (1)), are shown. As can be seen from the images, the shapes of the splats are also square. In Fig. 8(b), the FIB image of one of the YSZ splats, is shown. Most of the cavities between posts are filled in the middle, whereas, close to the boundaries of the splat, the cavities are partially empty.

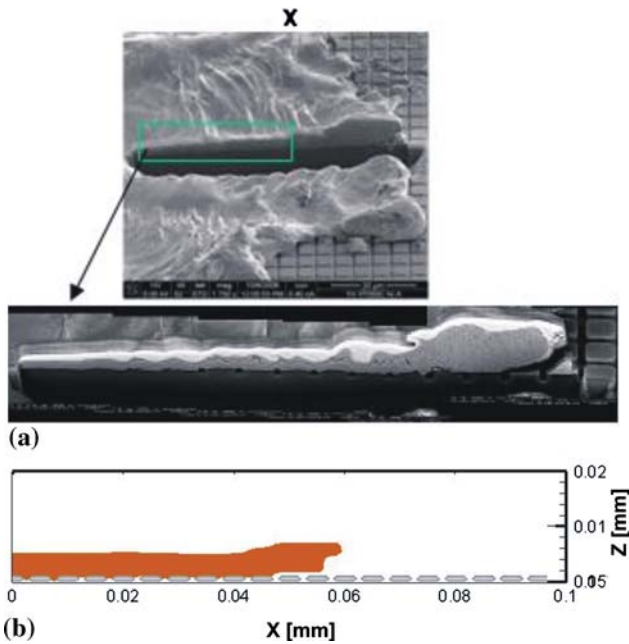


**Fig. 6** (a) FIB image from the nickel splat, corresponding to Fig. 2(a). The close-up of the cut shows that the posts close to the center of the splat are filled with material. The same feature can be seen from the simulation results, (b). (b) Cross sections of nickel splat, under same conditions at the location indicated by a line in Fig. 2(b)

As will be shown in the next section, the noncircular shape of the splat and its orientation (in this case, the splat's square edges are parallel to the rows of the posts) could be determined by the solidification parameters.

#### 4.3 Effect of Solidification on the Splat Shape

Raessi et al. (Ref 1) concluded from their simulations that droplet solidification is the main mechanism responsible for changing the splat shape. In this work, two different simulations of zirconia droplet impact on textured silicon, with the conditions presented in Table 2, columns (2) and (3), were performed. The simulations for two cases are called case (2) and case (3). The conditions for cases (2) and (3) are almost the same, except for two major differences. The initial temperature of the droplet in case (2) is 200 degrees less than that of the droplet in case (3). Also the thermal contact resistance used in simulations of case (2) is one order of magnitude higher than case (3). By decreasing the thermal contact resistance, the rate of heat transfer between the substrate and the splat is increased causing a more rapid solidification of the splat on the surface.

In Fig. 9(a) and (b), the simulation results for two cases of (2) and (3) are shown. The major difference that is quite obvious from the result is the difference between the orientations of the splats in two cases. In case (2), where the solidification is not considered to be rapid as case (3), the position of the splat and the pattern of the substrate are diagonal with respect to each other, whereas, in case (3), the splat orientation and the surface pattern are in the same direction.

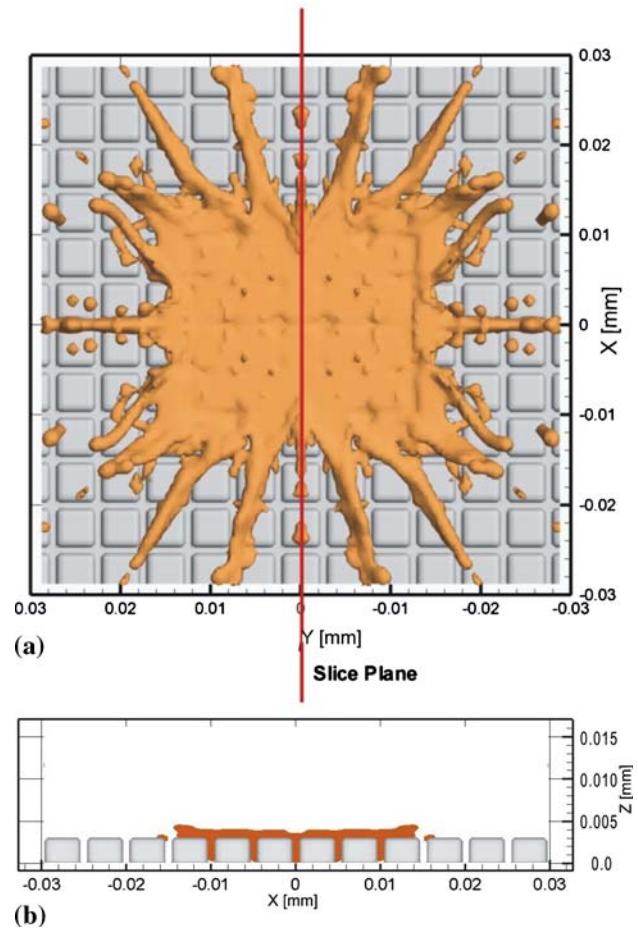


**Fig. 7** Numerical result for a YSZ splat on patterned silicon. The impact conditions and surface parameters are stated in Table 2. (a) The top view of the splat; (b) The cross section of the image at the location shown with a line in (a)

This phenomenon can also be seen from the SEM images of the actual molten zirconia droplets. In Fig. 10(a) and (b), the SEM images of zirconia splats on two different patterned surfaces are shown. Figure 10(a) shows the splat shape on a silicon wafer with a pattern of 3.3  $\mu\text{m}$  in height and 1  $\mu\text{m}$  spacing, whereas Fig. 10(b) shows the splat shape on a silicon wafer with a pattern of 1.5  $\mu\text{m}$  in height and 5.2  $\mu\text{m}$  spacing. The conditions of impacts are the same and as those stated for simulations of Fig. 9; Table 2, columns (2) and (3). Although the impact conditions for two droplets are the same, the different spacing between posts will affect the fluid movement as well as the thermal contact resistance between the substrate and the drop material. (By comparing the impact conditions of nickel droplets on two different patterned surfaces, increasing the space between the posts can decrease the thermal contact resistance, see Table 1.)

#### 4.4 Effect of Surface Roughness on Porosity of the Coating

One of the objectives of this study was to understand and also to characterize the effect of the substrate

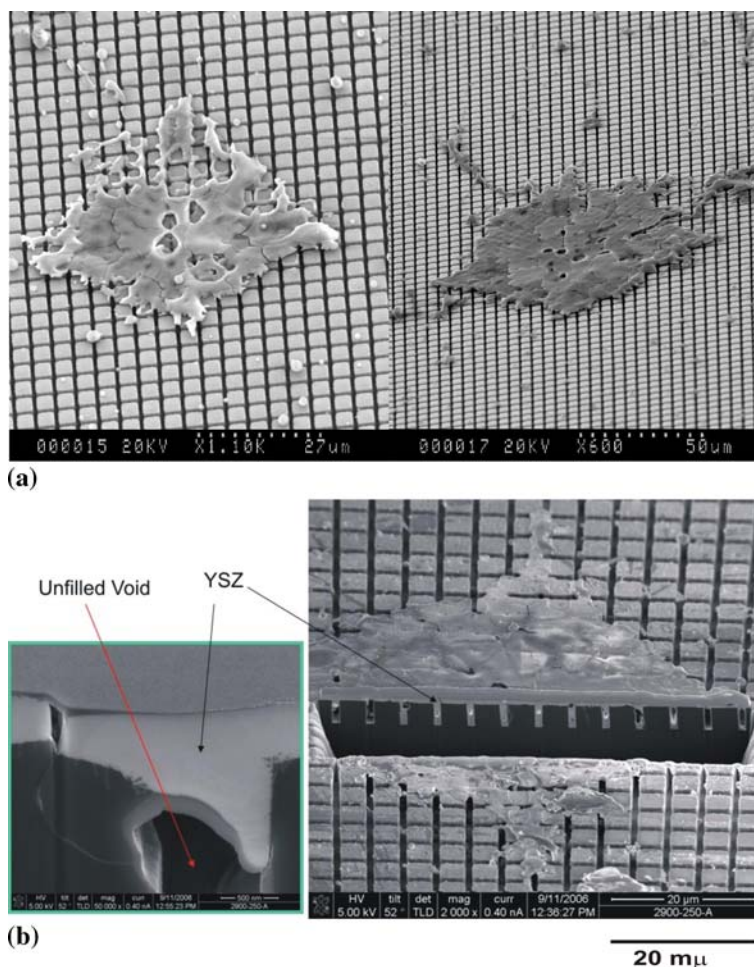


**Fig. 8** (a) Two SEM sample images from YSZ splats on patterned silicon surface. Please note the noncircular shapes of the splats. Impact conditions are as stated in Table 2, column (1). (b) The FIB image of a YSZ splat from the same experiment as (a). Spaces between roughness posts filled by YSZ except near edges of splat; YSZ bridges the posts

roughness parameters on the creation of the pores in the coating layers in thermal spray coating. As can be seen from the numerical simulations, which were also confirmed by most of the experimental results, the cavities of about  $3\ \mu\text{m}$  height on the surface is not completely filled with the drop material around the edges of the splats. This means that a percentage of pores in the coating layers close to the substrate may be caused by the existence of a rough substrate. Moreover, splashing around the splats and satellite droplets will create more rough areas that in turn create more porosity on the toping layers.

## 5. Conclusion

It was shown that the developed code is able to predict the dynamic behavior of the droplet impact on the patterned surface. The numerical simulation is shown to be a tool with a high potential for investigating the effect of

different parameters on the impact dynamic and solidification of the droplets.

Numerical simulations showed that the solidification rate affects the splat shape on a rough surface. Solidification rate is a function of thermal contact resistance between the splat and the substrate.

It was also shown that numerical simulation of single droplet impact on a well-defined patterned surface has the potential to be used for characterizing the pores' sizes and locations in the coating layers that result from unfilled cavities. The characterization is based on the initial drop and the impact conditions, as well as the roughness parameters of the surface. Recently, an analytical model has been developed to study the porosity formation mechanism in a coating layer and to predict the pore sizes based on the impact parameters. The method has been described in more details in (Ref 14) and has been implemented in software SimCoat (Ref 15).

The model can be extended beyond well-defined patterned surfaces, by importing the surface topology of a

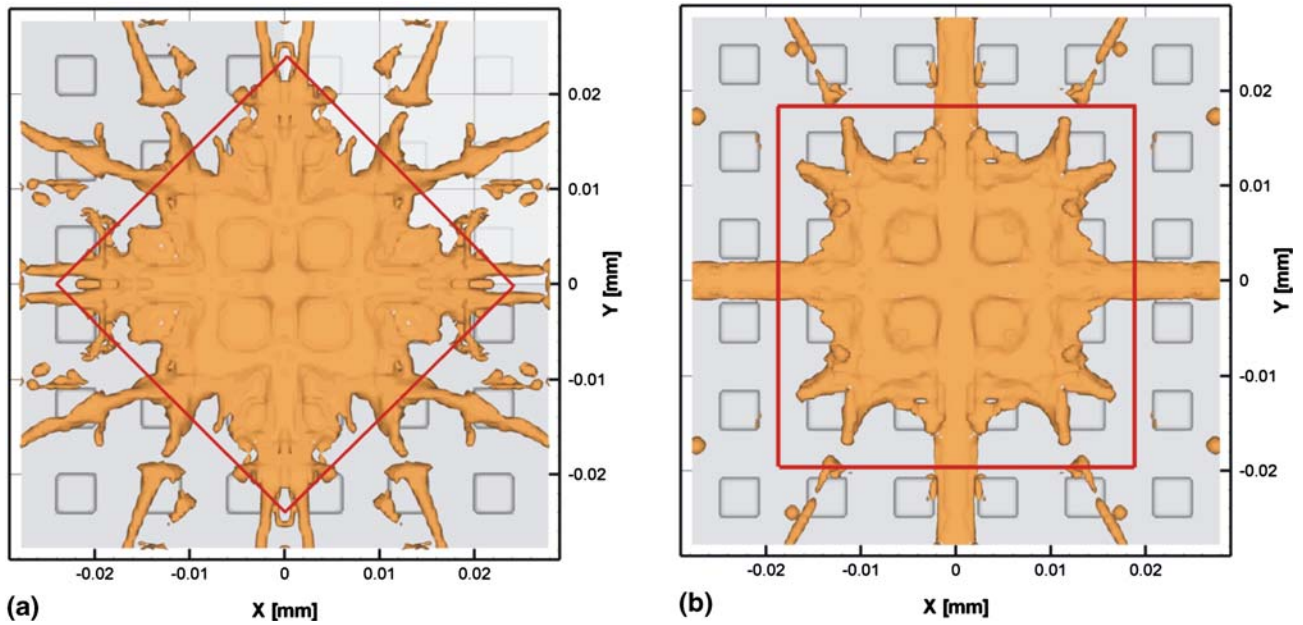


**Fig. 9** Simulation results for two zirconia splats. (a) Simulation conditions as in Table 2, column (2); (b) Simulation conditions as in Table 2, column (3)

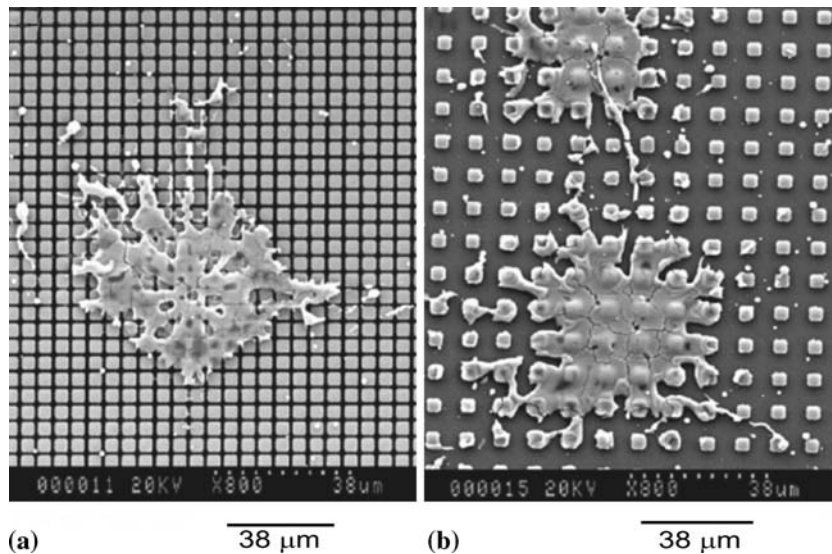


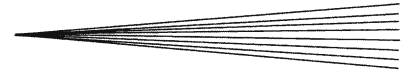
**Fig. 10** Single splats deposited on patterned Si: (a) Cube height 3.3  $\mu\text{m}$  and spacing 1  $\mu\text{m}$ ; (b) Cube height 1.5  $\mu\text{m}$  and spacing 5  $\mu\text{m}$  at room temperature. Particles' temperature and velocity are 2900  $^{\circ}\text{C}$  and 250 m/s, respectively

random patterned surface into the code, using a preprocessor. The uniform Cartesian cell sizes, then, can be determined by the size of the smallest peak on the surface.

## References

1. M. Raessi, J. Mostaghimi, and M. Bussmann, Droplet Impact During the Plasma Spray Coating Process – Effect of Surface Roughness on Splat Shapes, *Proceedings of 17<sup>th</sup> International Symposium on Plasma Chemistry*, J. Mostaghimi, T.W. Coyle, V.A. Pershin, and H.R. Salimi Jazi, Ed., August 7-12, 2005, (Toronto, Ontario, Canada), University of Toronto Press Inc., 2005, p 916-917
2. A.M. Ahmed and R.H. Rangel, Metal Droplet Deposition on Non-flat Surfaces: Effect of Substrate Morphology, *Int. J. Heat Mass Transfer*, 2002, **45**, p 1077-1091
3. H. Fukanuma, Mathematical Modeling of Flattening Process on Rough Surfaces in Thermal Spray, *Thermal Spray: Practical*





- Solutions for Engineering Problems*, C.C. Berndt, Ed., October 7-11, 1996 (Cincinnati, USA), ASM International, 1996, p 647-656
4. H. Liu, E.J. Lavernia, and R.H. Rangel, Modeling of Molten Droplet Impingement on a Non-flat Surface, *Acta Metall. Mater.*, 1995, **43**(5), p 2053-2072
  5. M. Bussmann, J. Mostaghimi, and S. Chandra, On a Three-Dimensional Volume Tracking Model of Droplet Impact, *Phys. Fluids*, 1999, **11**(6), p 1406-1417
  6. M. Pasandideh-Fard, S. Chandra, and J. Mostaghimi, A Three-dimensional Model of Droplet Impact and Solidification, *Int. J. Heat Mass Transfer*, 2002, **45**, p 2229-2242
  7. SimDrop is a software product of Simulent Inc., Toronto, Canada, <http://www.simulent.com>
  8. M. Raessi and J. Mostaghimi, Three-dimensional Modeling of Density Variation due to Phase Change in Complex Free Surface Flows, *Numer. Heat Transfer Part B – Fundamental*, 2005, **47**(6), p 507-531
  9. Y. Kawai and Y. Shiraishi, Ed., *Handbook of Physico-Chemical Properties at High temperature*, The Iron and Steel Institute of Japan, 1988
  10. K. Shinoda, Y. Kojima, and T. Yoshida, In Situ Measurement System for Deformation and Solidification Phenomena of Yttria-Stabilized Zirconia Droplets Impinging on Quartz Glass Substrate Under Plasma-Spraying Conditions, *J. Thermal Spray Technol.*, 2005, **14**(4), p 511-517
  11. D. Simon and U. Pal, Mathematical Modeling of a Melt Pool Driven by an Electron Beam, *Metall. Mater. Trans. B*, 1999, **30B**(3), p 517-526
  12. A. McDonald, "Visualization and Analysis of the Impact of Plasma-sprayed Particle," Ph.D. Thesis, University of Toronto, 2007
  13. A. McDonald, L. Rosenzweig, S. Chandra, and C. Moreau, Impact of Plasma-Sprayed Particles on Textured Silicon Wafers, *ILASS America*, Chicago, Illinois, May 2007
  14. M. Xue, Y. Heichal, S. Chandra, and J. Mostaghimi, Modeling the Impact of a Molten Metal Droplet on a Solid Surface Using Variable Interfacial Thermal Contact Resistance, *J. Mater. Sci.*, 2007, **42**, p 9-18
  15. SimCoat is a software product of Simulent Inc., Toronto, Canada, <http://www.simulent.com>